Pharm Res (2012) 29:972–982
DOI 10.1007/s11095-011-0637-9

RESEARCH PAPER

Prediction and *In Vitro* Evaluation of Selected Protease Inhibitor Antiviral Drugs as Inhibitors of Carboxylesterase 1: A Potential Source of Drug-Drug Interactions

Jenna A. Rhoades • Yuri K. Peterson • Hao-Jie Zhu • David I. Appel • Charles A. Peloquin • John S. Markowitz

Received: 12 September 2011 / Accepted: 21 November 2011 / Published online: 9 December 2011

ABSTRACT

Purpose To predict and determine whether the protease inhibitors (PIs) nelfinavir, amprenavir, atazanavir, ritonavir, and saquinavir could serve as metabolic inhibitors of the human CES1 (hCES1) using both molecular modeling techniques and *in vitro* inhibition assays.

Methods Initially, a molecular modeling approach was utilized to predict whether the selected PIs could serve as hCES1 inhibitors. The inhibitory effects of these PIs on hCES1 activity were then further evaluated utilizing previously established *in vitro* assay.

Results Pharmacophore and 2D-QSAR modeling predicted that nelfinavir would serve as a potent hCES1 inhibitor. This hypothesis was validated by *in vitro* hCES1 inhibition studies. Other PIs (amprenavir, atazanavir, ritonavir, saquinavir) were evaluated and also shown to be hCES1 inhibitors *in vitro*, although substantially less potent relative to nelfinavir.

Conclusion Computational molecular modeling is a valid approach to identify potential hCES1 inhibitors as candidates for further assessment using validated *in vitro* techniques. DDIs could occur when nelfinavir is co-administered with drugs metabolized by hCES1.

KEY WORDS carboxylesterase 1 · carboxylesterase 1 inhibitors · computational modeling · drug-drug interactions · *in vitro* inhibition · protease inhibitors

INTRODUCTION

Although curative treatments for human immunodeficiency virus (HIV) infection remain elusive, few antimicrobial agents or treatment regimens have had comparative impact to modern antiretroviral (ARV) medications in controlling what was previously an almost universally fatal infection (1). Indeed, ARVs have transformed HIV infection into a chronic yet manageable condition when properly utilized in patients compliant with treatment (2). Current treatment guidelines for HIV infection recommend the concurrent use of at least three ARV drugs for the treatment of HIV-infected patients in order to suppress viral replication thereby reducing the overall viral load (2). Additionally, combinatorial treatment approaches appear to delay the onset of resistance. In addition to the foundational

Electronic supplementary material The online version of this article (doi:10.1007/s11095-011-0637-9) contains supplementary material, which is available to authorized users.

J. A. Rhoades · H.-J. Zhu · D. I. Appel · C. A. Peloquin · J. S. Markowitz
Department of Pharmacotherapy & Translational Research
University of Florida
Gainesville, Florida, USA

Y. K. Peterson
Department of Pharmaceutical & Biomedical Sciences
Medical University of South Carolina
Charleston, South Carolina, USA

H.-J. Zhu · J. S. Markowitz
Center for Pharmacogenomics, University of Florida
Gainesville, Florida, USA

J. S. Markowitz (✉)
Department of Pharmacotherapy & Translational Research
Center for Pharmacogenomics
University of Florida College of Pharmacy
1600 SW Archer Road, RM PG-23
Gainesville, Florida 32610-0486, USA
e-mail: jmarkowitz@cop.ufl.edu

medications utilized in the treatment of HIV infection, patients generally receive concurrent pharmacotherapies targeted at common comorbid medical/psychiatric conditions in this patient population (e.g. cardiovascular disease, erectile dysfunction, and depression), including acute treatment and/or prophylaxis of opportunistic infections secondary to HIV infection, such as tuberculosis (3). Furthermore, there are well-documented adverse effects associated with the chronic use of many ARV therapeutic agents and regimens including hypertriglyceridemia, hypercholesterolemia, lipodystrophy, insulin resistance, and bone changes - all of which may be associated with a higher risk of developing long-term complications such as coronary artery disease (2,4,5). These conditions often require individualized pharmacotherapy as well. Thus, polypharmacy and the potential for drug-drug interactions (DDIs) are recognized as an almost inevitable consequence and risk associated with the current pharmacological management of the HIV patient, placing this population among the higher risk groups in terms of the potential for significant DDIs - even with vigilant monitoring. DDIs have become an increasingly complex challenge for clinicians treating patients with HIV infection (5).

Many combinations of ARVs lead to significant DDIs resulting in subtherapeutic or toxic drug concentrations and hence treatment failure (6). Most drug interactions associated with ARVs are mediated through either inhibition or induction of hepatic drug metabolism. Non-nucleoside reverse transcriptase inhibitors (NNRTIs) and PIs in particular, are known to influence the CYP450 system, particularly the CYP3A4 isoenzyme (7). Additionally, many ARVs are transported via ATP-binding cassette (ABC) membrane-associated efflux transporters as well as solute carrier (SLC) uptake transporters to varying degrees (6). Increasingly, the role of uridine diphosphate glucoronosyltransferase enzymes as well as nuclear receptor activation are being appreciated as mitigating factors in DDIs associated with ARV therapies (3,5). In comparison, there is essentially no published information regarding the potential contribution of the major hepatic hydrolases such as human carboxylesterase 1 (hCES1) to DDIs involving ARVs. Thus, the reality is that all potential and likely drug combinations prescribed to the HIV-infected patient simply cannot be addressed in product labeling or assessed in costly clinical studies designed to detect them. Accordingly, *in vitro* screening assays, while not without recognized limitations, remain valuable, rapid, and relatively inexpensive tools in the assessment of DDI potential (8).

In the present study, an assessment of the inhibitory capacity of a variety of PIs upon hCES1 activity was investigated. The hCES1 enzyme represents one of two major hepatic hydrolases (i.e. hCES1 and hCES2) contributing to approximately 80%–95% of total hydrolytic activity in the liver (9). hCES1 and hCES2, belonging to the classes CES1 and CES2, respectively, are currently viewed as the most relevant to drug metabolism in humans. Broad substrate specificities have been observed within hCES1 and hCES2 (9). Both are widely distributed throughout the body with the highest hydrolytic activity overall in the liver (10,11).

The PI nelfinavir was initially selected for screening to evaluate its capacity to inhibit hCES1 catalytic activity. Nelfinavir was specifically chosen based upon its prediction as a candidate inhibitor using an innovative computer modeling approach and algorithm at the study outset which is presented herein. Nelfinavir appeared as one of a number of therapeutic agents believed to contain the requisite pharmacophore to exert significant hCES1 inhibitory activity. Furthermore, the use of nelfinavir in a patient population already known to be at high risk for DDIs, and the relative dearth of information available pertaining to the influence of PIs on hydrolytic enzymes, provided additional impetus for assessing this compound. In the present study, a computational molecular modeling approach was utilized, optimized, and applied to the prediction of inhibitory effects of the PIs nelfinavir, amprenavir, atazanavir, ritonavir, and saquinavir on hCES1 activity. Furthermore, an established *in vitro* hCES1 inhibition assay was utilized to validate the predicted inhibition of the PIs on hCES1.

MATERIALS AND METHODS

Chemicals

dl-methylphenidate (*dl*-MPH), the internal standard, d_3-*dl*-methylphenidate (methyl labeled, *d3-dl*-MPH), *p*-nitrophenyl acetate (PNPA) and *p*-nitrophenol (PNP), were all purchased from Sigma-Aldrich (St. Louis, MO). The major *dl*-MPH metabolite formed *in vivo*, *dl*-ritalinic acid, was a gift from Dr. Kennerly S. Patrick (Dept of Pharmaceutical Sciences, Medical University of South Carolina). The protease inhibitors assessed included nelfinavir mesylate and amprenavir, atazanavir, ritonavir and saquinavir in free base form from Sequoia Research Products (Berkshire, UK). All other solvents as well as other agents employed in the preparation of assay buffers and other solutions were of the highest analytical grade commercially available.

Molecular Modeling of Potential hCES1 Inhibitors

Modeling, simulations and visualizations were performed using Molecular Operating Environment (MOE) Version 2010.10 (Chemical Computing Group Inc., Montreal,

Canada). Simulations were performed on a Dell E8500 with an Intel Core 2 Duo @ 3.16 GHz using a Windows XP OS. All other computational procedures were performed using a Dell XPS M1530 with an Intel Core2 Duo processor T8300@2.40 GHz w 2 GB RAM using a Windows Vista OS.

Pharmacophore Modeling

Structures of all screened compounds were analyzed using MOE software. Using tables of inhibitors incorporated as Simplified Molecular Input Line Entry Specification (SMILES) strings (which allow for the avoidance of ambiguity in the specification of a chemical structure via a text string) were imported into MOE as a mdb database. Molecule analysis was then performed using standard procedures. Molecules were rigidly aligned manually, and then subjected to MOE rigid body refinement (iteration limit 100, failure limit 20, energy cutoff 10). Consensus pharmacophores were calculated using specified thresholds, and the distance parameter (tolerance) was kept at the default value of 1.2 Å. Pharmacophore feature projections including Pi rings (PiN), H-bond acceptors (Don2), and H-bond acceptors (Acc2) were ignored in the analysis. Similarity was measured using the Tanimoto coefficient metric based on MACCS structural keys (*Maccs II*; Molecular Design Ltd., St, San Leandro, CA.)

The consensus pharmacophore represents the conserved features of 10 compounds and includes one additional feature from our previous work. F1 is a proton acceptor, F2 and F5 are a mixed-type feature, F3 and F4 are hydrophobic/aromatic features. Distances are F1-F2:7.65. F2-F3: 3.11. F3-F4 5.93, F4-F5 3.26, F1-F5:5.19, F1-F3: 6.22, F2-F4: 3.11, F2-F5: 3.15, and F3-F5: 4.12.

Pharmacophore Virtual Database Searching

The 4 point pharmacophore model was used to search the World Drug Index (WDI) database (2008). The WDI database contained 53,807 unique compounds representing drugs that have been tested in humans, and was used to create a 2,650,000 compound conformer library. Using the four point thioridazine model 125,491 conformers representing 17,921 compounds matched the model which in turn represents 33% of the database. It was not surprising that a significant percentage of the database was initially identified as possible substrates of hCES1, as the enzyme is known to be promiscuous and the model was built using small interacting compounds with a five feature model as input. It was therefore necessary to further analyze the hit list using an orthogonal prediction technique such as 2D-QSAR to improve the reliability of the absolute prediction.

2D-QSAR Modeling

Two 2-dimensional quantitative structure−activity relationship (2D-QSAR) models were built that showed significant predictive ability. In total 186 descriptors were calculated. Descriptors were trimmed to 152 in Model 1 and 154 in Model 2. QSAR modeling correlated activity as IC50 to the calculated 2D descriptors using the PLS regression method and cross-validation.

Computational Docking of HIV PIs to hCES1

The structural file used as input for analysis and docking simulations was pdb:1MX9 (12). Before analysis and simulations the hCES1 protein was protonated at pH 7.5 with a salt concentration of 0.2 M and structures energy minimized with heavy atoms constrained. Simulations focused on the enzyme active site determined by the location of morphine within pdb. Initial placement calculated 500 poses using triangle matching with London dG scoring; the top 250 poses were then refined using forcefield and ASE scoring. Initial placement calculated 500 poses using triangle matching with London dG scoring, the top 250 poses were then refined using forcefield and ASE scoring.

In Vitro Assessment of hCES1 Inhibition by PIs

A tiered approach was utilized in the evaluation of PIs wherein a generalized evaluation was initially performed using the model substrate PNPA to determine whether a given compound would impede hCES1 hydrolytic activity. This evaluation was then followed by more thorough and specific assay for identified inhibitors to specifically assess their potential for inhibiting hCES1 activity.

The establishment of cell lines over-expressing hCES1 as well as the cell s9 fraction preparation have been described in detail in previous reports (13,14). PNPA is a sensitive esterase substrate that is hydrolyzed to its major metabolite, PNP. The PNPA hydrolysis studies were performed in triplicate and carried out in 96-well culture plates at 37°C in a final volume of 200 µl. The s9 fraction from hCES1- and vector-transfected cells, the substrate PNPA, and the selected PIs for screening (nelfinavir, ritonavir, amprenavir, saquinavir, and atazanavir) were prepared in the assay buffer (Dulbecco's phosphate-buffered saline containing 10 mM HEPES, pH 7.4). The reaction was initiated by mixing s9 samples with PNPA and various concentrations of inhibitors. The final concentrations of the s9 proteins, tested compounds, and PNPA were 20 µg/ml, 100 µM, and 100 µM, respectively. After incubation at 37°C for 10 min, the formation of PNP from PNPA was determined by measuring absorbance at 405 nm. In the PNPA assay nelfinavir was found to

exhibit potent inhibition on hCES1-mediated PNPA hydrolysis, and was then subject to further study utilizing the selective hCES1 substrate *dl*-MPH. The hydrolytic activity of hCES1 was evaluated by determining the formation of the primary MPH metabolite, ritalinic acid. The experiment was conducted in 1.5 ml Eppendorf tubes in a total volume of 100 μL. After incubation of *dl*-MPH (0.1 μM) with 100 μg/ml s9 samples both in the presence and absence of nelfinavir (1, 3, 10, 30, 100 μM) at 37°C for 2 h, the hydrolytic reaction was terminated by adding 400 μl methanol containing the internal standard d3-*dl*-MPH (5 μg/ml). Reaction tubes were then subjected to centrifugation at 16,000×*g* for 10 min at 4°C. The hydrolytic metabolite of *dl*-MPH, ritalinic acid, formed via hCES1catalyzed de-esterification (i.e. hydrolysis) was quantified utilizing an established LC-MS/MS assay. This was carried out on a system consisting of a Shimadzu 10A HPLC system (Shimadzu, Tokyo, Japan) and an API 3000 triple quadrupole LC/MS/MS (Foster City, CA, USA).

Statistical Analysis

All data are presented as the mean ± SD. In the *in vitro* inhibition study, the IC_{50} is the concentration of inhibitor at which 50% of enzymatic activity is inhibited. The IC_{50} values were estimated by fitting the inhibition data to sigmoidal dose–response equation using GraphPad Prism 4.0 software (Intuitive Software for Science, San Diego, CA, USA). Statistical analysis was performed using one-way ANOVA and Dunnett's multiple comparison tests to compare PI-treated groups to control. The difference was considered significant when the *p*-value was less than 0.05.

RESULTS

Computer Modeling

We extend our previous hCES1 models to predict potential DDIs of clinical relevance. Using a thioridazine-based pharmacophore model and two thioridizaine-based 2D-QSAR models, we identified nelfinavir as a strong candidate molecule to produce hCES1 inhibition (Fig. 1). Our previous work described a four-point pharmacophore with a pharmacophore model of serving as an hCES1 chemotype based on thioridazine (13). The features include F1: proton acceptor, separated by a 2 carbon spacer where the next three features are derived from the dihydroanthracene backbone and include F2: hydrophobic or a proton acceptor, and F3/F4: hydrophobic or aromatic. These data were further refined using additional compounds from our previous work and those described in the literature (13,15,16). The refined pharmacophore contained one additional feature, F5, which is a promiscuous mixed-type hydrophobic proton acceptor/donor. This site contains the nitrogen from both 6- and 7-membered rings, and therefore is not in perfect alignment between the ring systems. Although this is a small model having only five features, it describes all of the conserved chemistry of the ligand set.

We used this pharmacophore to search the WDI database of known clinical drugs. The search required all four of the features matched with the sphere of chemical influence. Results were root-mean squared deviation to the dimensions of the model. Analysis of the results allowed us to further parse out from the list a number of widely prescribed medications identified as candidates. Figure 2 shows the graphical overlay results of a positive pharmacophore match.

Visual overlay of the top pharmacophore matches with the target clinical drug highlight the important chemical features for hCES1 interaction. It is interesting to note how dissimilar the actual chemical graphs appear between compounds like thioridazine, montelukast and nelfinavir yet their chemical features are nonetheless in tight correlation in chemical space.

Single cheminformatics models are not as powerful or accurate as consensus and/or combination of models (17). We therefore probed the results of the pharmacophore search using two different 2D-QSAR models (Fig. 3). The

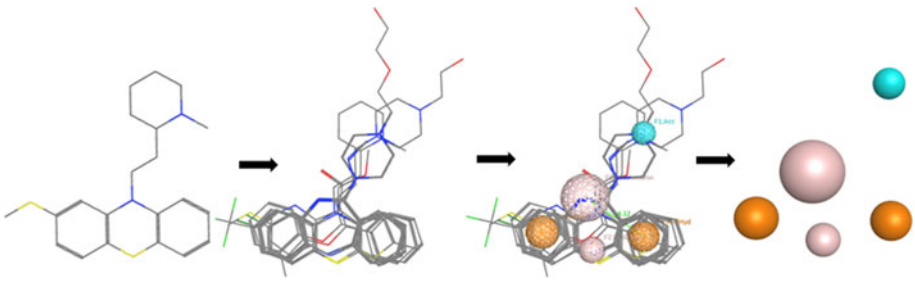

Fig. 1 Alignment and generation of a thioridazine class specific hCES1 pharmacophore. The first panel depicts thioridazine. The second panel depicts the alignment of multiple hCES1 interacting molecules with chemcial similarity to thioridazine. The third panel depicts the multiple alignment with pharmacophore features overlaid. The Fourth panel depicts the derived pharmacophore alone. Moieties are: proton acceptors in blue, hydrophobic and aromatic in orange, and mixed type features in pink.

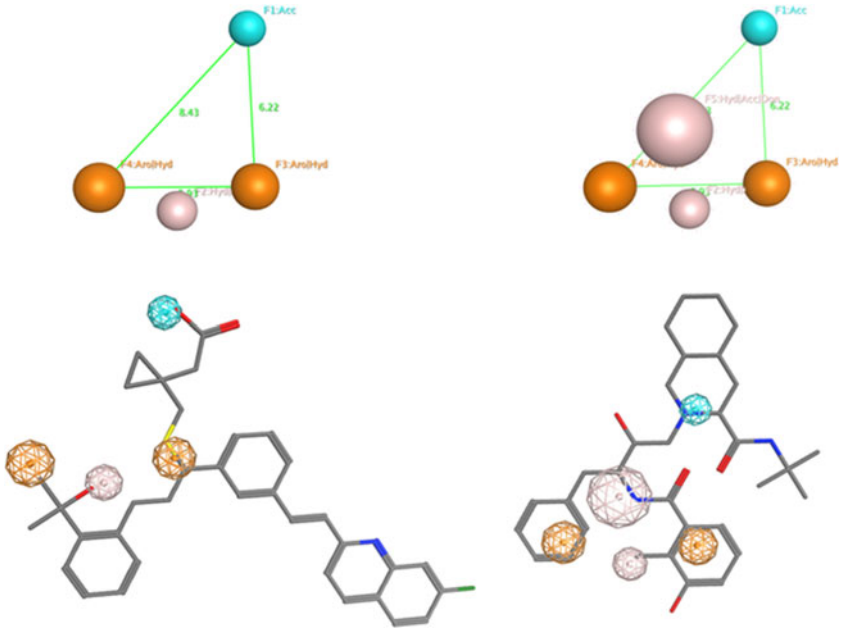

Fig. 2 Comparison of four *versus* five point thioridazine type pharmacophore models. Overlay of the 4- and 5-point pharmacophore model with both montelukast and nelfinavir highlighting chemical matches to thioridazine. Moieties are: proton acceptors in blue, hydrophobic in green, and aromatic in orange.

2D-QSAR models were built from a multitude of known hCES1 inhibitors (Supplemental Table 1).

Analysis of the top descriptors used in the 2D-QSAR model can provide insight into the chemical properties that may be indicative of a potentially significant inhibitor of hCES1. Also as noted by others, weight, which is analogous to mass in the case of the QSAR model descriptor, is consistently ranked as a top descriptor (Supplemental Table 2). While correlation of weight with activity would normally provide very little useful information, correlation of the descriptor with structural information from the docking simulations indicates that the size of the active-site pocket within hCES1 is limited in volume and will exclude or prevent conformational flexibility of large compounds. An upper boundary appears to be near 600 Da

Although all of the PIs tested share structural similarities, significantly different effects on hCES1 catalytic efficiency between the agents were noted. Nelfinavir, which, *a priori*, was predicted to be the most potent hCES1 inhibitor, was confirmed to be the most potent hCES1 inhibitor *in vitro*. At 85% similarity by MAACS keys, all the PIs are unique. At 65% similarity there are three groups where nelfinavir and amprenavir are singletons and saquinavir, ritonavir and atazanavir are clustered together. At 60% similarity all of the compounds cluster together with the lone exception of amprenavir. The compounds exhibit a wide range of physiochemical properties. Notably, nelfinavir has the lowest radius and highest logP value (Fig. 4).

We further extend the predictive model of hCES1 inhibition and present data on the interaction of other

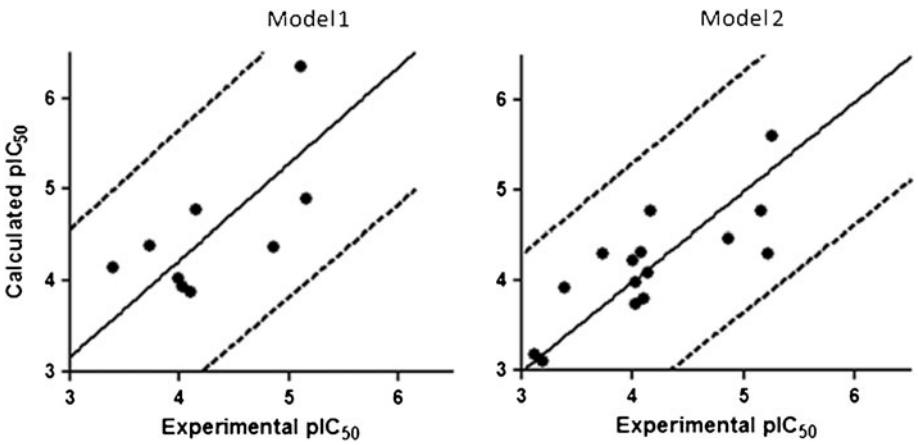

Fig. 3 Correlation regression for 2D QSAR models used to predict novel hCES1 inhibitors. For both graphs the data represent the experimental activity *versus* the cross-validated QSAR prediction of activity. The solid line is the linear regression forced through origin (R_o^2). The dotted line represents the 95% prediction band.

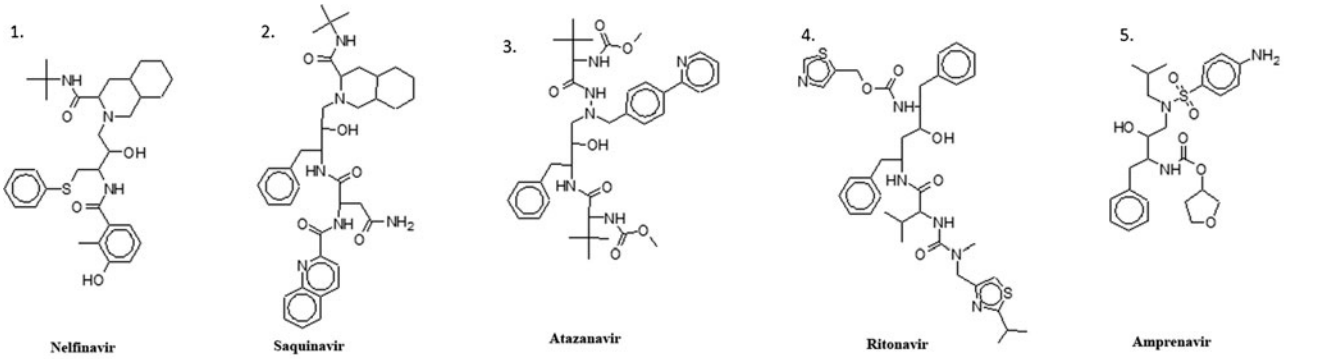

name	Weight	diameter	weinerPath	vsa_hyd	SlogP_VSA7	vdw_vol	logP(o/w)	85%CLUSTER	65%CLUSTER	SMILES
nelfinavir	567.8	14	5398	444.6	141.1	796.9	5.4	1	1	S(C[C@H](NC(=O)c1cccc(O)c1C)[C@H](O)CN1CC2C(C[C@H]1C(=O)NC(C)(C)C)CCCC2)c1ccccc1
sasquinavir	670.9	19	9512	464.2	198.8	932.6	3.3	2	2	O=C(N[C@@H](CC(=O)N)C(=O)N[C@H]([C@H](O)CN1CC2C(C[C@H]1C(=O)NC(C)(C)C)CCCC2)Cc1ccccc1)c1nc2c(cc1)cccc2
ritonavir	721.0	22	10769	556.2	224.8	968.1	5.0	3	2	s1cncc1COC(=O)N[C@@H](Cc1ccccc1)C(O)C[C@@H](NC(=O)C(NC(=O)N(Cc1nc(sc1)C(C)C)C)C(C)C)Cc1ccccc1
atazanavir	704.9	19	10532	556.1	234.9	979.6	4.7	5	2	O(C(=O)N[C@@H](C(C)(C)C)C(=O)N[C@H]([C@@H](O)CN(NC(=O)[C@@H](NC(OC)=O)C(C)(C)C)Cc1ccc(cc1)-c1ncccc1)Cc1ccccc1)C
amprenavir	505.6	15	3813	356.3	158.8	666.1	2.4	4	4	S(=O)(=O)(N(CC(C)C)C[C@@H](O)[C@@H](NC(O[C@H]1CCOC1)=O)Cc1ccccc1)c1ccc(N)cc1

Fig. 4 HIV protease inhibitors and their properties. (Top) The hydrogen suppressed chemical graphs of the five major HIV protease inhibitors are depicted. (Bottom) The pharmacophore and QSAR model prediction values and physiochemical properties are listed.

widely utilized drugs that significantly interact with hCES1. One such drug is the leukotriene receptor antagonist montelukast, widely used in the prophlyaxis and chronic treatment of asthma as well as the prevention of exercise-induced bronchoconstriction. Montelukast was found to be one of the potent hCES1 inhibitors tested with an IC_{50} value of 7.8±4.5 μM determined by PNPA hydrolysis assay.

In order to better understand the mechanism of PI inhibition of hCES1 we performed a series of ligand-enzyme interaction simulations using computational docking (Fig. 5). In this case the active site of hCES1 (pdb 1MX9) was used as a rigid probe for the flexible interaction of PIs (12). Nelfinavir was consistently a top-scoring dock hit, and had the highest ranking of all the PIs assessed. In fact, the docking simulations were in exact agreement with the rank order of potencies determined in *in vitro* assays, essentially providing a cross-validation for both experiments. Mean docking scores were between −30 and −25, indicating a strong predicted interaction. Saquinavir had the largest amount of conformational flexibility with the hCES1 active site while amprenavir had the least. This is not unexpected as the flexibility of the inhibitors can be rationalized by the mass and number of rotatable bonds within the compound.

Analysis of the binding modes of the predicted nelfinvir-hCES1 interaction indicated a mix of hydrogen bonding and hydrophobic interactions (Fig. 6). Only one hydrogen bond was predicted in the top scoring neflinavir pose, with Leucine 4304 being a proton acceptor with an amide of nelfinavir. Hydrophobic interactions predominated the interactions with large numbers of hydrophobic residues from hCES1 interacting with nelfinavir (Ala 93, Leu 97, Phe 101, Val 146, Val 254, Leu 318, Leu 358, Ile 359, Leu 363,Met 364, Leu 388, Phe 426, and Met 425) interacting with the hydrophobic moieties of neflinavir (phenyl, trimethyl, and isoquinoline). In fact, the hydrophobic moieties of nelfinavir are saturated by hydrophobic amino acid interactions. A comparison of the nelfinavir interaction with the opiate morphine suggests that many of the same amino acids are critical, but the binding mode is different (Fig. 6). In particular these are hydrophobic amino acids creating a small hydrophobic pocket, designed to sample

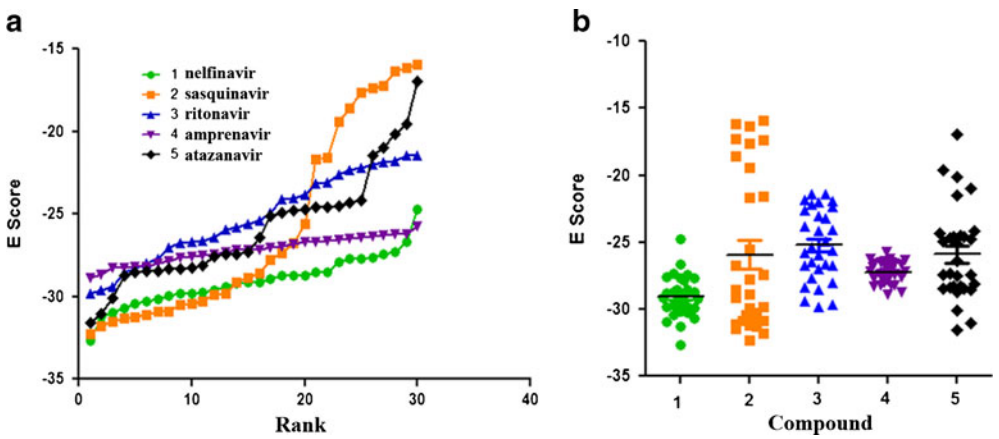

Fig. 5 Docking simulation analysis of HIV PIs interaction with hCES1. (**a**) Rank ordered docking hits from the top 30 refined docking hits to the active site of hCES1 (pdb 1MX9). For docking simulations 50 poses were refined to 30 and analyzed for low docking E scores. (**b**) Histogram of docking hits from (**a**).

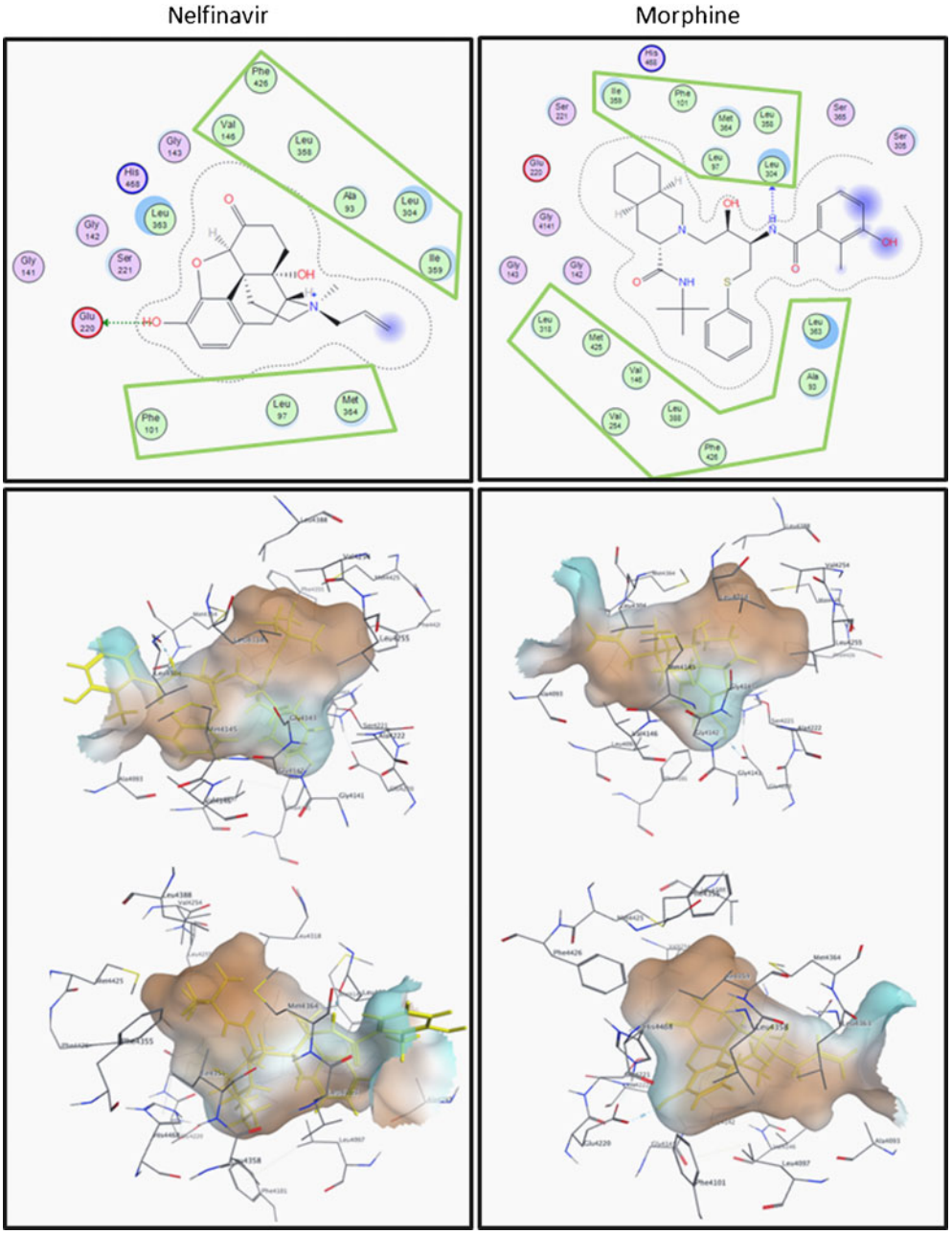

Fig. 6 Analysis of the hCES1 active site interactions with nelfinavir *versus* morphine. Top panels: Interactions diagram showing hydrogen bonding depicted as arrows, hydrophobic residues colored in green, and clusters of hydrophobic residues boxed. Bottom Panels: The internal active site pocket of hCES1 is imaged along with the representative substrate colored in yellow with the pocket colored brown representing hydrophobicity and blue representing hydrophilicity.

the local environment and partition small hydrophobic xenogens. These data are in agreement with recently published data on the physiochemical requirements for hCES1 interactions with morphine and heroin, which indicate a relationship of affinity with hydrophobicity. Additionally, these results allude to an upper mass boundary where compounds with very large acyl/alkyl/aryl groups are not CES substrates despite being generally hydrophobic (15,18).

Nelfinavir occupies a larger percentage of the active site than morphine, and might indicate a higher affinity of hCES1 for nelfinavir then morphine. However, the terminal hydroxymethylbenzene of nelfinavir might counteract the increased active-site interactions by providing access to the bulk solvent.

In Vitro Inhibition of hCES1 Activity by Selected Protease Inhibitors

The PNPA incubation studies indicated that each PI exhibited varying degrees of inhibition of hCES1-mediated PNPA hydrolysis (Fig. 7). The hCES1 activity towards PNPA hydrolysis was determined to be 5.2±3.0%, 74.2±1.6%, 51.7±1.7%, 76.9±5.2%, 67.8%±8.3%, respectively, of the control after co-incubation with 100 μM of nelfinavir, ritonavir, amprenavir, saquinavir, and atazanavir.

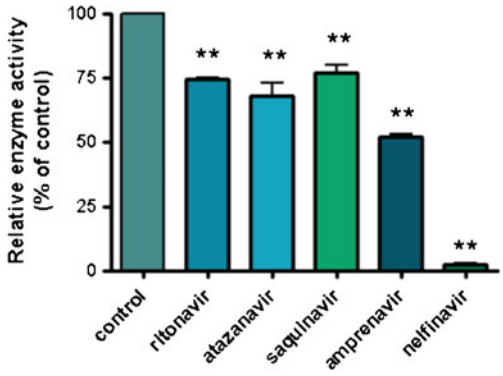

Fig. 7 Inhibition of hCES1-mediated PNPA hydrolysis by the PIs nelfinavir, ritonavir, amprenavir, saquinavir, and atazanavir. The relative hCES1 activity in control group was defined as 100%. The data are the means from 3 independent experiments with error bars representing SD. $^{**}p < 0.01$ *versus* control.

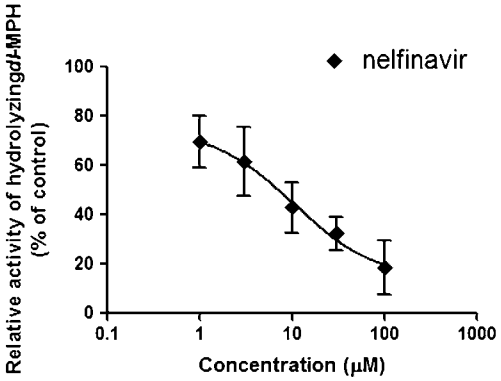

Fig. 9 The inhibitory effect of nelfinavir on *dl*-MPH hydrolysis catalyzed by hCES1. hCES1 activity was assessed by determining the formation of the hydrolytic metabolite of *dl*-MPH, ritalinic acid. Data are presented as the mean ± SD of three independent experiments.

Nelfinavir was found to be the most potent inhibitor with a Ki value of 3.7±0.7 μM determined by PNPA hydrolysis assay (Fig. 8). The inhibition kinetic study revealed that nelfinavir did not alter the V_{max} value of hCES1-catalyzed PNPA hydrolysis, but increased the K_m value, indicating that nelfinavir inhibited hCES1 via a competitive mechanism (Fig. 8). Nelfinavir was further assessed for hCES1 inhibition utilizing the selective hCES1 substrate *dl*-MPH. The results demonstrate that nelfinavir inhibited *dl*-MPH hydrolysis mediated by hCES1 in a concentration-dependent manner with an IC_{50} value of 6.6±4.0 μM (Fig. 9).

DISCUSSION

The management of patients with HIV has become increasingly complex, with DDIs frequently a consequence of combined medication regimens. Clinician awareness and education with regard to drugs associated with clinically significant DDIs, including ARVs, is a critical and ongoing process as new data continue to emerge relevant to DDIs in this at-risk patient population.

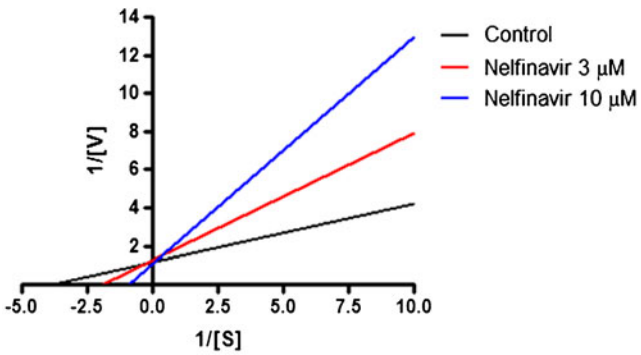

	control	3μM	10μM
Vmax	863.0 ± 42.4	800.0 ± 17.8	915.5 ± 34.5
Km	264.5 ± 46.4	532.0 ± 36.0	1082.0 ± 100.8

Fig. 8 Kinetic study of nelfinavir's inhibitory effects on hCES1-mediated PNPA hydrolysis. The incubation of nelfinavir resulted in the increase of K_m without altering the V_{max}, indicating nelfinavir inhibited PNPA hydrolysis via a competitive mechanism.

hCES1 is the major hydrolytic enzyme governing the biotransformation of a large and diverse group of therapeutic agents including *dl*-MPH, oseltamivir, various angiotensin-converting enzyme (ACE) inhibitors and others. Metabolism via hCES1 can yield either inactive metabolites, as in the case of the MPH hydrolytic metabolite ritalinic acid, or alternatively, active metabolites, as in the case of the activation of the anti-influenza prodrug oseltamivir phosphate to its active form oseltamivir carboxylate. Significant interindividual variability of pharmacokinetic and pharmacodynamic profiles of these medications has been consistently observed in clinical practice, which was associated with unexpected adverse drug reactions and the failure of pharmacotherapy. It has been demonstrated that the variation of hCES1 expression and activity is one of the major contributing factors influencing therapeutic outcomes of the drugs metabolized by hCES1. *CES1* genetic variation, developmental expression and DDIs are considered the main causes of the interindividual variability of hCES1 function. Several *CES1* variants were found to be associated with altered hCES1 activity and expression (14). Consequently, the patients who carry these functional *CES1* mutations exhibited varied responses to hCES1 substrate drugs relative to their wild-type peers. *In vitro* studies have shown that hepatic hCES1 expression is markedly lower in individuals under 1 year of age, and increases gradually, suggesting that particular caution should be observed when known hCES1 substrate drugs are prescribed to younger pediatric patients (19). Beyond functional genetic variants and developmental age, hCES1-mediated DDIs are increasingly recognized for their potential contribution

to the variability of tolerability and response of many medications.

Previously published studies from our laboratory and others have identified a number of routinely prescribed medications and a variety of natural health products as potential inhibitors of hCES1 (13,20,21). However, the present study differs in its approach and rationale for compound selection for assessment in its use and refinement of a molecular modeling approach to identify selected clinically used agents as candidates for screening. Both *in vitro* and animal studies have indicated that significant DDIs could occur after co-administration of hCES1 inhibitors with hCES1 substrates such as *dl*-MPH. We also demonstrated that computational molecular modeling is a valid approach for initial identification of potential hCES1 inhibitors. A combination of both pharmacophore and QSAR models provided sufficient detail to accurately predict hCES1 inhibitor activity. The pharmacophore model of thioridazine type hCES1 inhibitors provides a discrete way to map functionalities critical to hCES1 interaction onto molecules with unrelated chemical graphs. This unique ability of pharmacophore modeling is exemplified by the thioridazine pharmacophore mapping onto both monetleukast and nelfinavir, all three being distinct chemical species. Combination of both pharmacophore and QSAR modeling to analyze the same dataset allowed enrichment of a potential test set from 17,921 compounds (WDI) to 65, or 0.5% of the database. Both QSAR modeling and docking simulations indicated and confirmed previous studies that the size and hydrophobicity of the interacting drug is critical for effective interaction. The top descriptors for the QSAR models were molecular weight and molecular volume and hydrophobicity descriptors. Docking simulations and analysis of the hCES1 active site indicated affinity was roughly correlated with molecular weight for the HIV protease inhibitors tested. Using morphine as a model, it is shown that PIs take up increasing amounts of the limited volume within the hCES1 active site and the active site interactions are primarily hydrophobic. Interestingly, the mass cutoff for effective hCES1 interaction is very near the Lipinski upper mass cutoff for small molecules of 500 Da. This generalized chemistry is indicative of the promiscuous nature of hCES1 and the plethora of interacting drugs speaks to its clinical importance. Besides identification of known drugs with affinity for hCES1, these models will be useful for prediction of novel drugs as they move down the drug development pipeline. These data provide potential insight to a structural-mechanistic basis for hCES1 inhibition and pertinent information regarding the cross-reactivity of a number of clinical medications. Essential features for hCES1 interaction include a combination of hydrophobic and hydrogen bonding moieties while keeping the structure within a limited total mass. The hCES1 active site is planar, indicating that planar molecules may have a better chance of effectively interacting with the enzyme. Our pharmacophore model culled 35,887 compounds from the WDI data base that might otherwise be considered candidates for screening. Obviously, such a screening would be a massive undertaking and would not be realistic in terms of resources and time constraints for most laboratories but does translate into a significantly decreased number of molecules as potential candidates to test hCES1 inhibitory activity. When the pharmacophore model was combined with a QSAR model, we were able to further reduce the number of candidate molecules to assess by 53,742 representing 99.5% of the database, an even greater increase in efficiency in terms of focused our screening efforts.

Consistent with the prediction of our molecular modeling, *in vitro* inhibition study confirmed that nelfinavir is a potent hCES1 inhibitor, whereas other selected PIs are weaker hCES1 inhibitors relative to nelfinavir. The maximum plasma concentrations of nelfinavir in HIV positive patients receiving typical doses of nelfinavir were reported to range from 1 to 4 μg/ml (22,23), which is in the same range of the Ki and IC_{50} values determined in the present *in vitro* studies. Thus, it appears likely that nelfinavir could reach a level sufficient to inhibit hCES1 activity *in vivo*, though free drug concentrations of nelfinavir in the liver is unknown.

The limitations of *in vitro* assays and models with regard to extrapolating such findings to the *in vivo* situation have been well described. Certainly issues of drug absorption, plasma protein binding, tissue distribution, excretion and others can influence the overall disposition of a compound. With these limitations borne in mind, only cautious speculation is possible regarding potential clinical impact of our findings. The present situation is further complicated in that hCES1 inhibition as a mechanism of DDIs is a possibility few researchers and far fewer clinicians may consider relative to its potential role in DDIs. Furthermore, in the case of hCES1-catalyzed hydrolytic reactions of specific prodrugs, the focus is largely upon subsequent oxidative metabolism mediated by the CYP450 system following the liberation of the active drug via de-esterification. In the case of nelfinavir and other PIs, there is wide recognition of the risk of DDIs via potent inhibition of CYP3A4. Thus, in the case of some documented DDIs producing metabolic inhibition, there may be an unrecognized contribution from hCES1 as well as CYP3A4. For example, the 3-hydroxy-3-methylglutaryl coenzyme A (HMG-CoA) reductase inhibitors ("statins") are frequently co-administered with ARV therapies as a result of dyslipidemia arising from a PI-induced metabolic disturbance. It is well known that PI treatment can lead to significant elevations in plasma concentrations of a number of statin drugs. However, it is noteworthy that among the

statins, simvastatin, a prodrug requiring initial de-esterification by hCES1 to release the active hydroxyl acid compound, is profoundly increased (>500-fold increase in AUC and Cmax) with nelfinavir co-administration (24, 25) and this may place patients at risk of statin-induced rhabdomyolysis, believed to be a concentration-dependent adverse effect possibly resulting in fatality (26). It has been suggested that simvastatin be avoided altogether in combination with PI therapy (24). Although all are potentially problematic, the degree of elevation in plasma concentrations of other HMG-CoA reductase inhibitors such as pravastatin and atorvastatin (which are not prodrugs or hCES1 substrates) is not nearly of the magnitude observed with simvastatin. Thus, in theory, the possibility exits that in addition to CYP3A4 inhibition by nelfinavir, an additional contribution via hCES1 inhibition may lead to these dramatic increases. Nevertheless, such scenarios remain speculative and in need of confirmation through future *in vivo* studies. It should be noted that hCES1 as a mechanism of DDIs is an area in its infancy relative to other extensively studied enzyme systems such as CYP450.

It is noteworthy that, beyond catalyzing the metabolism of therapeutic agents, hCES1 is also involved in lipid metabolism, in which hCES1 is alternatively referred to as triacylglycerol hydrolase (TGH). Decreased plasma triacylglycerol, apolipoprotein B, and fatty acid levels have been observed in TGH knock-out mice in both fasted and fed states (27). Thus, it is of interest to elucidate whether the use of hCES1 inhibitors could result in the alternation of lipid metabolism in humans, particularly in view of the known association between PI use and the development of dyslipidemias.

In summary, we have demonstrated that computational molecular modeling could serve as a valuable tool to predict which therapeutic agents may serve as hCES1 inhibitors and hence, a source of potential DDIs. Nelfinavir, initially predicted as a hCES1 inhibitor from our molecular models, was confirmed to exhibit potent and competitive inhibitory effect on hCES1 using an established *in vitro* assay. It appears plausible that hCES1-mediated DDIs could occur when nelfinavir is co-administered with other medications predominantly metabolized by hCES1, but this must be verified through conduct of *in vivo* studies.

REFERENCES

1. Volberdingand PA, Deeks SG. Antiretroviral therapy and management of HIV infection. Lancet. 2010;376:49–62.
2. Thompson MA, Aberg JA, Cahn P, Montaner JS, Rizzardini G, Telenti A, Gatell JM, Gunthard HF, Hammer SM, Hirsch MS, Jacobsen DM, Reiss P, Richman DD, Volberding PA, Yeni P, Schooley RT. Antiretroviral treatment of adult HIV infection: 2010 recommendations of the International AIDS Society-USA panel. JAMA. 2010;304:321–33.
3. Marzolini C, Elzi L, Gibbons S, Weber R, Fux C, Furrer H, Chave JP, Cavassini M, Bernasconi E, Calmy A, Vernazza P, Khoo S, Ledergerber B, Back D, Battegay M. Prevalence of comedications and effect of potential drug-drug interactions in the Swiss HIV Cohort Study. Antivir Ther. 2010;15:413–23.
4. Hawkins T. Understanding and managing the adverse effects of antiretroviral therapy. Antiviral Res. 2010;85:201–9.
5. Pauand AK, Boyd SD. Recognition and management of significant drug interactions in HIV patients: challenges in using available data to guide therapy. Clin Pharmacol Ther. 2010;88:712–9.
6. Kis O, Robillard K, Chan GN, Bendayan R. The complexities of antiretroviral drug-drug interactions: role of ABC and SLC transporters. Trends Pharmacol Sci. 2010;31:22–35.
7. AIDSinfo. Guidelines for the Use of Antiretroviral Agents in HIV-1-Infected Adults and Adolescents. http://aidsinfonihgov/Guidelines/GuidelineDetailaspx?GuidelineID=7&ClassID=1 (2011).
8. Grimm SW, Einolf HJ, Hall SD, He K, Lim HK, Ling KH, Lu C, Nomeir AA, Seibert E, Skordos KW, Tonn GR, Van Horn R, Wang RW, Wong YN, Yang TJ, Obach RS. The conduct of *in vitro* studies to address time-dependent inhibition of drug-metabolizing enzymes: a perspective of the pharmaceutical research and manufacturers of America. Drug Metab Dispos. 2009;37:1355–70.
9. Imai T, Taketani M, Shii M, Hosokawa M, Chiba K. Substrate specificity of carboxylesterase isozymes and their contribution to hydrolase activity in human liver and small intestine. Drug Metab Dispos. 2006;34:1734–41.
10. Satoh T, Taylor P, Bosron WF, Sanghani SP, Hosokawa M, La Du BN. Current progress on esterases: from molecular structure to function. Drug Metab Dispos. 2002;30:488–93.
11. Fleming CD, Bencharit S, Edwards CC, Hyatt JL, Tsurkan L, Bai F, Fraga C, Morton CL, Howard-Williams EL, Potter PM, Redinbo MR. Structural insights into drug processing by human carboxylesterase 1: tamoxifen, mevastatin, and inhibition by benzil. J Mol Biol. 2005;352:165–77.
12. Bencharit S, Morton CL, Xue Y, Potter PM, Redinbo MR. Structural basis of heroin and cocaine metabolism by a promiscuous human drug-processing enzyme. Nat Struct Biol. 2003;10:349–56.
13. Zhu HJ, Appel DI, Peterson YK, Wang Z, Markowitz JS. Identification of selected therapeutic agents as inhibitors of carboxylesterase 1: potential sources of metabolic drug interactions. Toxicology. 2010;270:59–65.
14. Zhu HJ, Patrick KS, Yuan HJ, Wang JS, Donovan JL, DeVane CL, Malcolm R, Johnson JA, Youngblood GL, Sweet DH, Langaee TY, Markowitz JS. Two CES1 gene mutations lead to dysfunctional carboxylesterase 1 activity in man: clinical significance and molecular basis. Am J Hum Genet. 2008;82:1241–8.
15. Hatfield MJ, Tsurkan L, Hyatt JL, Yu X, Edwards CC, Hicks LD, Wadkins RM, Potter PM. Biochemical and molecular analysis of carboxylesterase-mediated hydrolysis of cocaine and heroin. Br J Pharmacol. 2010;160:1916–28.
16. Zhu HJ, Markowitz JS. Activation of the antiviral prodrug oseltamivir is impaired by two newly identified carboxylesterase 1 variants. Drug Metab Dispos. 2009;37:264–7.
17. Nagao Y, Ishitobi Y, Kinoshita H, Fukushima S, Kawashima H. YM175, a new bisphosphonate, increases serum 1,25-dihydroxyvitamin D in rats via stimulating renal 1-hydroxylase activity. Biochem Biophys Res Commun. 1991;180:1172–8.
18. Vistoli G, Pedretti A, Mazzolari A, Testa B. In silico prediction of human carboxylesterase-1 (hCES1) metabolism combining docking analyses and MD simulations. Bioorg Med Chem. 2010;18:320–9.

19. Zhu HJ, Appel DI, Jiang Y, Markowitz JS. Age- and sex-related expression and activity of carboxylesterase 1 and 2 in mouse and human liver. Drug Metab Dispos. 2009;37:1819–25.
20. Takahashi S, Katoh M, Saitoh T, Nakajima M, Yokoi T. Different inhibitory effects in rat and human carboxylesterases. Drug Metab Dispos. 2009;37:956–61.
21. Liu R, Tam TW, Mao J, Saleem A, Krantis A, Arnason JT, Foster BC. The effect of natural health products and traditional medicines on the activity of human hepatic microsomal-mediated metabolism of oseltamivir. J Pharm Pharm Sci. 2010;13:43–55.
22. Hirt D, Mentre F, Tran A, Rey E, Auleley S, Salmon D, Duval X, Treluyer JM. Effect of CYP2C19 polymorphism on nelfinavir to M8 biotransformation in HIV patients. Br J Clin Pharmacol. 2008;65:548–57.
23. Read JS, Best BM, Stek AM, Hu C, Capparelli EV, Holland DT, Burchett SK, Smith ME, Sheeran EC, Shearer WT, Febo I, Mirochnick M. Pharmacokinetics of new 625 mg nelfinavir formulation during pregnancy and postpartum. HIV Med. 2008;9:875–82.
24. Fichtenbaum CJ, Gerber JG, Rosenkranz SL, Segal Y, Aberg JA, Blaschke T, Alston B, Fang F, Kosel B, Aweeka F. Pharmacokinetic interactions between protease inhibitors and statins in HIV seronegative volunteers: ACTG Study A5047. AIDS. 2002;16:569–77.
25. Hsyu PH, Schultz-Smith MD, Lillibridge JH, Lewis RH, Kerr BM. Pharmacokinetic interactions between nelfinavir and 3-hydroxy-3-methylglutaryl coenzyme A reductase inhibitors atorvastatin and simvastatin. Antimicrob Agents Chemother. 2001;45:3445–50.
26. Hare CB, Vu MP, Grunfeld C, Lampiris HW. Simvastatin-nelfinavir interaction implicated in rhabdomyolysis and death. Clin Infect Dis. 2002;35:e111–2.
27. Wei E, Ben Ali Y, Lyon J, Wang H, Nelson R, Dolinsky VW, Dyck JR, Mitchell G, Korbutt GS, Lehner R. Loss of TGH/Ces3 in mice decreases blood lipids, improves glucose tolerance, and increases energy expenditure. Cell Metab. 2010;11:183–93.